On the bonding situation in $TlCo_2Se_2$

2006 J. Phys.: Condens. Matter 18 1757

(http://iopscience.iop.org/0953-8984/18/5/027)

INSTITUTE OF PHYSICS PUBLISHING JOURNAL OF PHYSICS: CONDENSED MATTER

J. Phys.: Condens. Matter **18** (2006) 1757–1768 doi:10.1088/0953-8984/18/5/027

On the bonding situation in $TlCo_2Se_2$

M V Yablonskikh[1,4], R Berger[2], U Gelius[3], R Lizárraga[3], T B Charikova[4], E Z Kurmaev[4] and A Moewes[1]

[1] Department of Physics and Engineering Physics, University of Saskatchewan, 116 Science Place, Saskatoon, Saskatchewan S7N 5E2, Canada
[2] Department of Materials Chemistry, Ångström Laboratory, Uppsala University, Box 538, SE-75121 Uppsala, Sweden
[3] Department of Physics, Ångström Laboratory, Uppsala University, Box 530, SE-75121 Uppsala, Sweden
[4] Institute of Metal Physics, Russian Academy of Sciences—Ural Division, 620219 Yekaterinburg, Russia

E-mail: iablonskikh@usask.ca and rberger@mkem.uu.se

Received 30 November 2005, in final form 3 January 2006
Published 20 January 2006
Online at stacks.iop.org/JPhysCM/18/1757

Abstract

The electronic structure of $TlCo_2Se_2$ has been investigated by means of band structure calculations and x-ray photoelectron and emission spectroscopy (XPS and XES). The formation of the valence band is described in connection with calculations of partial densities of states of the valence band and Co $L_{\alpha,\beta}$ x-ray emission ($3d4s \rightarrow 2p_{3/2}, 2p_{1/2}$) aligned to the binding energy scale. The experimental results are in agreement with the calculated distribution of Co 3d states, which lie close to the Fermi level. The effect of Co–Se bonding is seen as satellite structures in the XPS Co 2p signals. Thermoelectric and Hall effect data as well as resistivity measurements show that $TlCo_2Se_2$ is metallic with electron holes as charge carriers with broadband mobility characteristics. The observed anisotropy of the resistivity in the ab plane and along c remains constant as a function of temperature, i.e. without signs of the magnetic ordering that occurs ($T_N \sim 85$ K). The results of local spin density functional calculations show ferromagnetic coupling within the cobalt plane as a result of direct magnetic interactions between the magnetic moments.

1. Introduction

The $ThCr_2Si_2$-type family compounds are interesting due to large variations in magnetic and transport properties depending on element choice on the three crystallographic positions in $I4/mmm$ [1–3]. In this structure type of general stoichiometry AT_2X_2, the T atoms (transition metals) form layers, each one being a square network with the possibility of short-range interactions between atoms within each sheet. The distance between the layers is increased for

large X atoms as compared to the more common p-elements, such as silicon and phosphorus. The distance between the layers is also increased further if the A atom is large, for instance a fairly heavy atom with a low oxidation state. Therefore, the two-dimensional character is further accentuated by the choice of A = K, Rb, Cs, Tl and Ba, and X = S, Se and Te. Thallium representatives were first more systematically synthesized by Klepp and Boller [4]. They suggested a larger ionic contribution, formally as $Tl^{+}T_2X_2^{-}$ with (X = S, Se), in contrast to the more common alloy representatives.

The alloys $TlCu_2X_2$ (X = S, Se, Te) have been studied regarding electrical transport properties [5–7], and the magnetic effects of substitution on the T site were investigated [5, 6]. Berger and van Bruggen correlated various physical properties to the pronounced two-dimensional character of these phases, also relating to the concentration of charge carriers [6, 8]. This thread was picked up by Greenblatt and co-workers [1, 9–11] who worked extensively on similar solid solutions including the title compound studied further here.

The reason for a more detailed study of $TlCo_2Se_2$ is, first of all, that the renewed interest in the solubility of copper in it [12, 13] also resulted in a more detailed knowledge of the character of the magnetic interactions [3, 14]. Instead of classical collinear antiferromagnetism [1], an incommensurate spin spiral was found [14]. Details of the electronic structure were gained earlier from calculations [3, 15]. A second reason for this study is that the two isostructural compounds $TlCo_2Se_2$ and $TlCo_2S_2$, both having a strong two-dimensional character and differing chemically only as regards the X atom, show quite different magnetic ordering schemes on cooling. The sulfide orders ferromagnetically with $T_C \sim 150$ K [9, 11, 16]. To obtain experimental element-specific band structure information we chose x-ray emission and x-ray photoelectron spectroscopy and compare the measurements to our DOS calculations. Electron transport measurements complement the results and show the character of the charge carriers. Our aim being to shed light on the differences in binding properties between $TlCo_2Se_2$ and $TlCo_2S_2$ that is reflected in the contrasting magnetic properties.

2. Experimental details

Single crystal material was obtained from slowly cooling a melt of the appropriate composition [1]. Various thin flakes could be sliced from a highly textured ingot. Such flakes were used for spectroscopic studies as well as for transport property measurements. The direction normal to a flake face was ⟨001⟩, the face being of the form {0 0 1}.

2.1. X-ray photoelectron spectra (XPS)

The instrument used for the XPS studies was a Scienta ESCA-300 spectrometer [17] with a monochromatized Al Kα x-ray excitation source. The $TlCo_2Se_2$ crystal was mechanically mounted on a standard sample holder, and adhesive tape was pressed onto the available upper crystal surface. We used the same instrument and followed the same procedure as that already reported [16] for a crystal of the analogous $TlCo_2S_2$, stripping the crystal face in UHV in the preparation chamber. Only a small percentage of the crystal surface was imperfect since it contained some tiny circular dents, leaving small holes in the peeled off layers on the tape. These are probably the result of gaseous inclusions during crystal growth.

The UHV-peeled crystal was then transferred to the analysis chamber and placed onto a universal manipulator. The electron emission angle relative to the surface was chosen to be 90° in order to make the XPS analysis as bulk sensitive as possible. The lateral and polar orientations of the crystal were optimized, seeking to minimize the O 1s and C 1s line intensities that emanated from the unstripped circular dents and possible residues of tape glue.

Survey spectra ($0 \rightarrow 1000$ eV, 500 eV pass energy) and detailed spectra, including the valence band ($22 \rightarrow -3$ eV, 300 eV pass energy), were recorded for three different UHV-cleaved surfaces, showing different amounts of O 1s and C 1s contaminations. The spectra from the best cleavage gave almost identical Co 2p, Se 3d, Tl 4f and valence-band spectra as the second best cleavage that had only slightly higher O 1s and C 1s signals. The energy calibration of the instrument was made versus the Ag $3d_{5/2}$ peak of silver metal at 368.27 eV.

For comparison, a piece of cobalt metal (99.98%) was scraped in UHV, and a survey spectrum as well as 2p and 3p spectra were recorded. The O 1s and C 1s signals were hardly detectable.

2.2. Resonant x-ray emission spectra (RXES) and x-ray absorption spectra (XAS)

The x-ray fluorescent measurements were performed at the soft x-ray fluorescence end-station located on beamline 8.0.1 at the Advanced Light Source (ALS) at Lawrence Berkeley National Laboratory. The emitted radiation was measured using a Rowland-circle-type spectrometer with spherical gratings and a multichannel plate detector [18]. To reduce the effect of surface contamination, the sample was filed in vacuum (1×10^{-6} Torr) before measurements. The reference cobalt metal was not filed, resulting in slight surface oxidation evident from the Co $L_{3,2}$ absorption.

X-ray absorption spectra (XAS) of Co in $TlCo_2Se_2$ were measured in total fluorescence and total electron yield modes (TFY and TEY respectively) with the monochromator resolution set to 0.1 eV.

For the resonant x-ray emission measurements, the energy resolution for the exciting radiation was set to 0.2 eV. The Co $L_{\alpha,\beta}$ spectra were recorded using an energy resolution of about 0.8–0.9 eV, as estimated. For energy calibration of x-ray spectra we used reference spectra of the metals calibrated according to values taken from Bearden [19].

2.3. Electrical transport

The single crystal used in the investigation was $4.8 \times 2 \times 0.1$ mm^3 in size. The contacts for the electrical resistivity measurements were soldered to the samples using a silver paste annealed at 570 K for 3 h. Standard four-terminal measurements of the resistivity and Hall effect ($j \parallel ab, B \parallel c$) in the dc regime in an automated setup were carried out in the temperature range $4.2\ \text{K} \leqslant T \leqslant 300$ K without a magnetic field and in a magnetic field $B = 1$ T, respectively.

Thermoelectricity data were collected on cooling from room temperature to the He boiling point with the help of a commercial setup (SB 100/NMR Technologies) using proprietary software and copper leads against a copper/constantan reference.

2.4. Density of states (DOS) calculations

The full-potential augmented plane wave method with local orbitals [20, 21] was used together with the local spin density approximation (LSDA) as parameterized by von Barth and Hedin [22] to calculate the DOS for a spin-spiral state as determined experimentally [14], i.e. for the propagation vector $\mathbf{Q} = [0, 0, 0.7]2\pi/c$. The structural as well as the convergence parameters, such as the number of k-points, number of basis functions and the temperature broadening, were kept as in [15]. The calculated moment by this approach was 0.51 μ_B/Co.

Additionally, the details of the ferromagnetic DOS calculated by the full-potential plane wave method, as implemented in the WIEN2k code [23, 24], are presented here. The exchange–correlation energy has been treated within the generalized gradient approximation (GGA) after

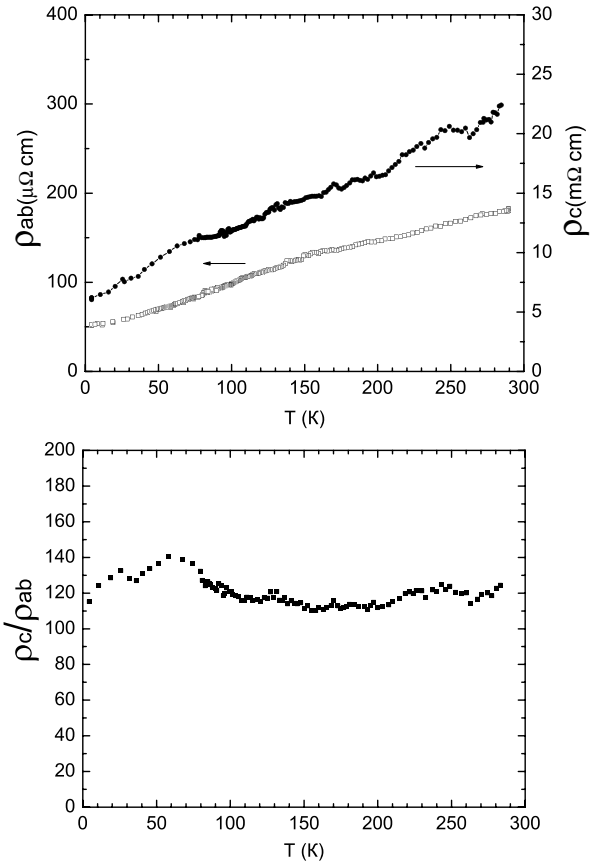

Figure 1. Resistivity measurements of $TlCo_2Se_2$. Top frame: measurements performed in the ab plane and along the c direction are presented on different scales; the left and right arrows show the scale for a specific plot. Bottom frame: illustration of the resistivity ratio versus temperature.

Perdew, Burke and Ernzerhof [25]. The DOS was calculated for the ferromagnetic structure of $TlCo_2Se_2$ in the body-centred tetragonal lattice, space group $I4/mmm$. The lattice constants are $a = 3.8315$ Å, $c = 13.4250$ Å from low-temperature diffraction [14]. A k-mesh of $8\times8\times8$ in combination with muffin-tin sphere radii of 2.2 au (Tl) and 2.1 au (Co, Se) was used. The local magnetic moment within the Co atomic sphere is 0.78 μ_B.

3. Results and discussion

3.1. Transport properties

The temperature dependence of the electrical resistivity ρ of a $TlCo_2Se_2$ single crystal measured in the ab plane in the range 4.2 K $\leqslant T \leqslant$ 300 K indicates that the phase is highly metallic; see figure 1. The $\rho(T)$ dependence is close to linear, which is similar to what has been observed previously [1]. The thermal variations of the anisotropy ρ_c–ρ_{ab} are found to be small, at least above the Néel temperature (86 K). However, the data of the resistivity along the c-axis were rather difficult to obtain and the variations in the anisotropy ratio get artificially magnified. The magnetic moments are oriented within the ab plane [3, 14, 15].

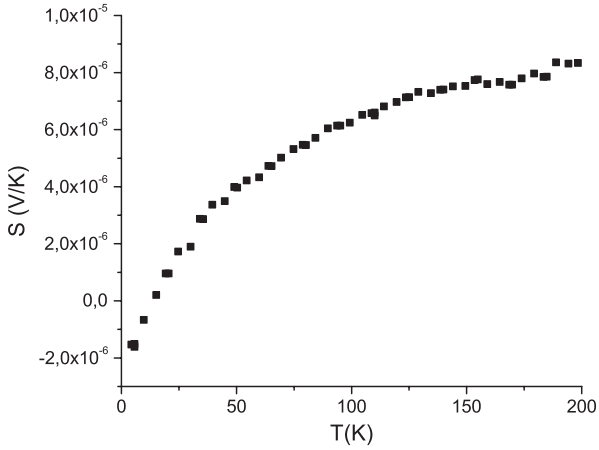

Figure 2. Seebeck coefficient of $TlCo_2Se_2$ versus temperature.

The Hall-effect measurement at $T = 4.2$ K showed a positive Hall constant $R_H = 1.4 \times 10^{-3}$ cm^3 C^{-1}, indicating that the charge carriers are holes. Considering the cell parameters at this temperature ($a = 3.833$ Å, $c = 13.43$ Å from [14]), the hole concentration $p \approx 4.5 \times 10^{21}$ cm^{-3} translates into 0.45 holes/formula unit—disregarding any anomalous contribution, since there is no net magnetic moment. A value for the carrier mobility may be obtained by combining the Hall-effect and resistivity data. However, ρ (at 4 K) is 5×10^{-5} Ω cm in our measurement and 3×10^{-4} Ω cm in that of [1]. Those figures give a mobility of 30 and 5 cm^2 V^{-1} s^{-1}, respectively. In either case, such a value is typical for broad bands.

The presence of holes in the valence band is supported by the thermoelectric data, which show a positive Seebeck coefficient (S) of a very low magnitude (see figure 2). The temperature dependence is very similar to that of $TlCu_2Se_2$ of the same structure type [6], possibly related to the form of the Fermi surface. There is a linear relationship between S and temperature only at higher temperatures, the slope being 1.5×10^{-8} V K^{-2}. A similar value was found for $TlCu_2Se_2$, quite in line with the expectations for a broadband conductor [6].

3.2. X-ray spectra and DOS calculations

The best survey spectrum of the XPS studies is shown in figure 3. It is noteworthy that the O 1s and C 1s peaks are very small. No other contaminants were detected. The total amount of oxygen and carbon contamination for these samples must be less than 5 at.%. Since the valence electrons in the investigated valence-band region ($\leqslant$22 eV binding energy) of carbon and oxygen have lower photoionization cross-sections [26] than the valence electrons of the other elements, their intensity contribution to the valence-band region and to other spectra is totally negligible. Noteworthy features within this energy range are the sharp Tl $5d_{3/2}$ and $5d_{5/2}$ peaks.

We have compared measured XPS spectra with ones taken for the isostructural compound $TlCo_2S_2$ [16] and also for cobalt metal itself. It is found that the spectra of Tl 4f, Tl 5d and of Co 2p are very similar irrespective of chalcogen atom. Values for the peaks are collected in table 1. The Co 2p spectrum shown in figure 4 has no significant energy shift as compared to that of metallic cobalt [27] and they are very similar, which supports the metallic character of the bonding. The extra spectral structures occurring approximately 2.5 eV higher in

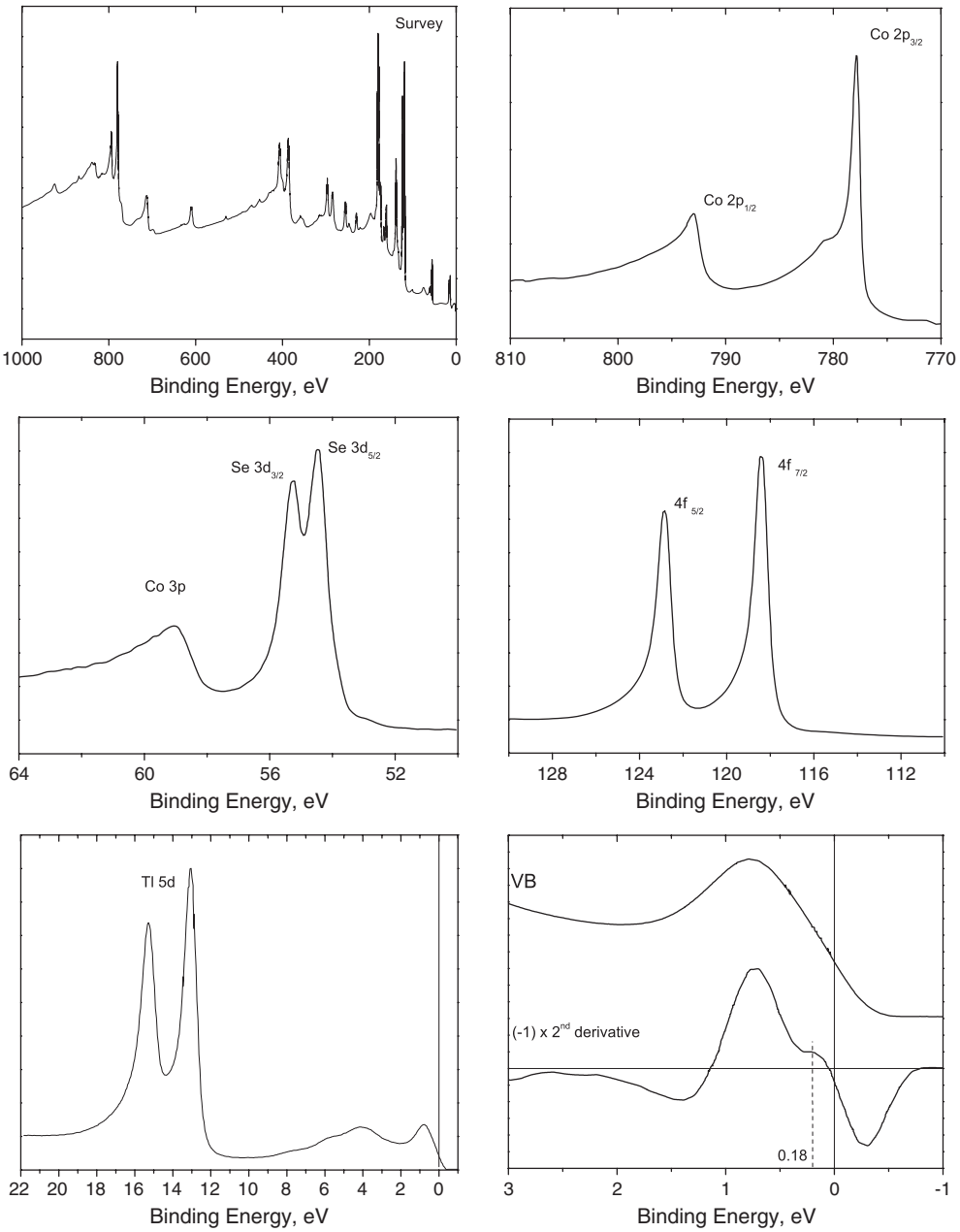

Figure 3. XPS spectra of $TlCo_2Se_2$. Survey spectrum (top left), Co 2p (top right), Se 3d and Co 3p (bottom left), and Tl 4f (bottom right). The intensities are given on a relative scale. The horizontal axes show the binding energies in eV units, where zero corresponds to the Fermi energy. Bottom-left frame: XPS valence-band spectrum, including thallium bands and Fermi-edge states. Bottom-right frame: the second derivative with reversed sign is included for a more detailed profile analysis.

binding energy than the $2p_{3/2}$ core level peak, and to a lesser extent as a low-energy shoulder, are attributed to Auger effects [28] but might also contain some information on the Co–X bonding (X = S, Se).

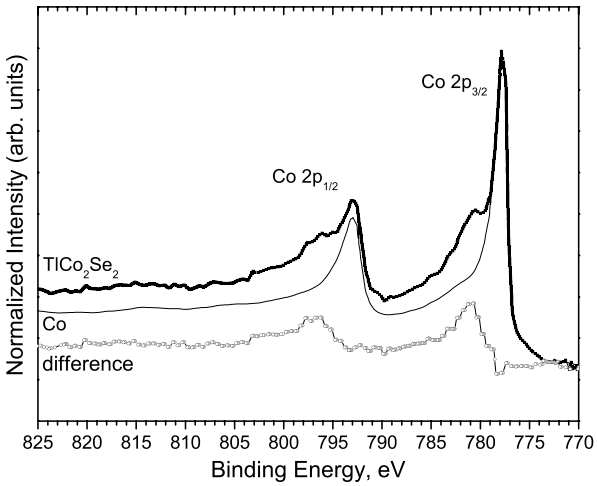

Figure 4. XPS spectra of $TlCo_2Se_2$ (see figure 3) and cobalt metal in the Co 2p region, as well as their difference (dotted curve).

Table 1. Selected experimental binding energy data in units of eV for $TlCo_2Se_2$ from XPS compared to $TlCo_2S_2$ [16]. (Calibration against silver metal Ag $3d_{5/2}$ at 368.27 eV.)

Core electron level	$TlCo_2Se_2$	$TlCo_2S_2$
Tl $5d_{5/2}$	13.10	13.16
Tl $5d_{3/2}$	15.35	15.42
Tl $4f_{7/2}$	118.37	118.40
Tl $4d_{5/2}$	122.81	122.85
Co 3p	59.15	
Co $2p_{3/2}$	777.95	778.15
Co $2p_{1/2}$	792.96	793.17
Se $3d_{5/2}$	54.42	
Se $3d_{3/2}$	55.28	

Also, cobalt metal shows anomalies at the 2p peaks and even at Co 3s, likely due to multiplet effects [29]. An attempt for a detailed analysis of the extra Co 2p features was made by scaling the spectra from $TlCo_2Se_2$ and cobalt metal and then taking their difference. By this procedure, the effects of the overlapping Auger signals are supposed to be taken care of, considering that these should be the same in the two spectra. The difference curve shows (figure 4) very clearly that there are distinct satellite features to both 2p peaks, most likely due to the Co–Se bonding. The energy difference between these weak peaks is roughly the same as the spin–orbit splitting between the main peaks, and the relative intensities also reflect their connection to these.

The Co $L_{\alpha,\beta}$ ($3d \rightarrow 2p_{3/2}$, $3d \rightarrow 2p_{1/2}$) RXES of $TlCo_2Se_2$ are shown in figure 5. The $L_{\alpha,\beta}$ RXES does not exhibit any difference between the Co bonded in the sample and the cobalt metal reference. The shape of all of them is metallic-like, proving a largely metallic electronic structure of cobalt in $TlCo_2Se_2$. These data, and the tailing asymmetry characteristic of all detail spectra of XPS, confirm the metallic behaviour of the compound as also verified by the electrical transport measurements.

Almost identical features appear in the corresponding Co 2p XPS spectrum of $TlCo_2S_2$ [16]. They indicate that the bonding situation about Co is only subtly sensitive to

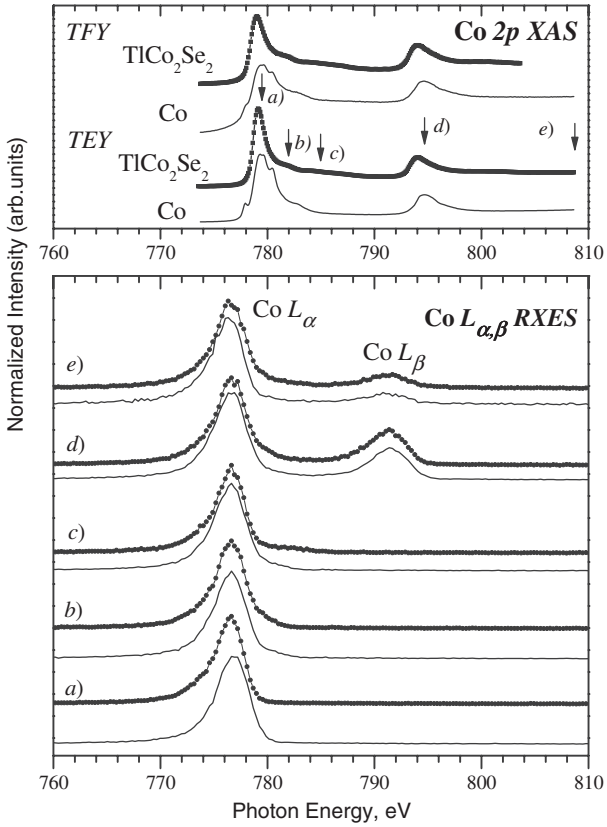

Figure 5. Co $L_{2,3}$ x-ray absorption and Co $L_{\alpha,\beta}$ resonant x-ray emission spectra. The data of $TlCo_2Se_2$ are plotted with bold dots while the $L_{\alpha,\beta}$ spectra of the cobalt metal reference are plotted with a thin solid line. The upper panel shows Co 2p x-ray absorption spectra measured in total electron yield (TEY) and total fluorescence yield (TFY) mode. The arrows correspond to selected excitation energies labelled from (a) to (e), and found with the same labelling in the Co $L_{2,3}$ RXES displayed in the lower panel. The extra features in the XAS spectra of the cobalt metal are due to superficial CoO. Please note the reversal in energy scaling direction compared to the XPS spectra.

the identity of the X atom (see table 1). Still more striking is the fact that not even the valence-band spectra differ very much, except that the hump just below the Fermi edge has a maximum of 0.8 eV for the selenide and 1.0 eV for the sulfide. For both alloys extra shouldering is seen at a binding energy of roughly 0.2 eV. In comparison with the valence-band spectrum of $TlCo_2S_2$ [16] the one of $TlCo_2Se_2$ is less pronounced and may be found using the second derivative (figure 3). It is mostly due to the photoionization cross-section of Se (0.26×10^{-2}) which is approximately a factor of 2.6 larger than that of S (0.1×10^{-2}) [26]. The shoulder at 0.18 eV is predicted by calculations of $g(E)$ and its convolution $p(E)$ in which the photoionization cross-sections were taken into account (figure 6). However, the XPS experiment was performed at room temperature, which is above the ordering temperature. Moreover, XPS represents an excited atomic state while the calculations are to be valid for $T = 0$ K, where magnetic ordering is established.

The valence-band structure displayed in figure 6 is understood from comparison of XES and XPS with DOS calculations, also shown in a spin-polarized form in figure 7 (taking care of the ferromagnetic interactions within the cobalt layers). The Fermi level cuts the top of the

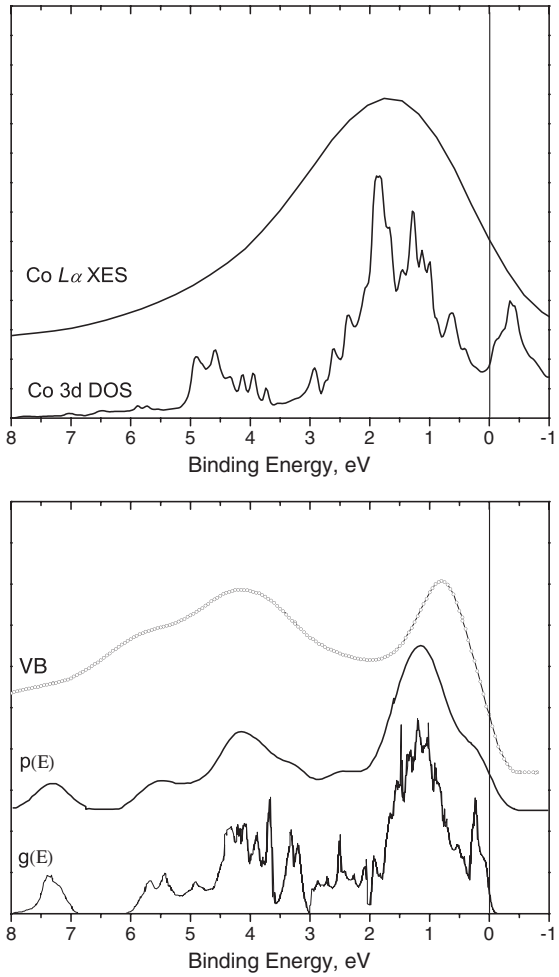

Figure 6. Top frame: corresponding overlay between DOS calculations and the Co L_α non-resonant x-ray emission spectrum (figure 5), aligned to the binding energy scale using the Co $2p_{3/2}$ core level energy taken from XPS measurements. Bottom frame: measured valence-band spectrum (VB, see figure 3), calculated density of states $g(E)$ for a spin spiral, and its convolution $p(E)$ with cross-sections and instrumental broadening in the valence-band regime.

valence band which is in line with the metallic properties of the compound. We were able to identify the energy of Co 3d states in the valence band, which, according to XES aligned using the Co 2p binding energy [30], to its largest part is 1–2 eV below the Fermi level. There is quite good agreement with the DOS calculations. When comparing the DOS calculations with the XPS VB spectrum, the calculated data were convoluted by spectral broadening and the effects of different cross-sections. The main agreement is striking; the position of the main maximum differs only by 0.3 eV.

The total DOS of the ferromagnetic spin-polarized situation has been subdivided into partial contributions by the three elements (see figure 7). These features may also be expressed into partitioning onto specific bonds, as a crystal orbital Hamilton population (COHP) (for details about COHP see [16] and references therein). However, such data are not presented here but are extremely similar to the situation in $TlCo_2S_2$, computed by LMTO [16]. The main

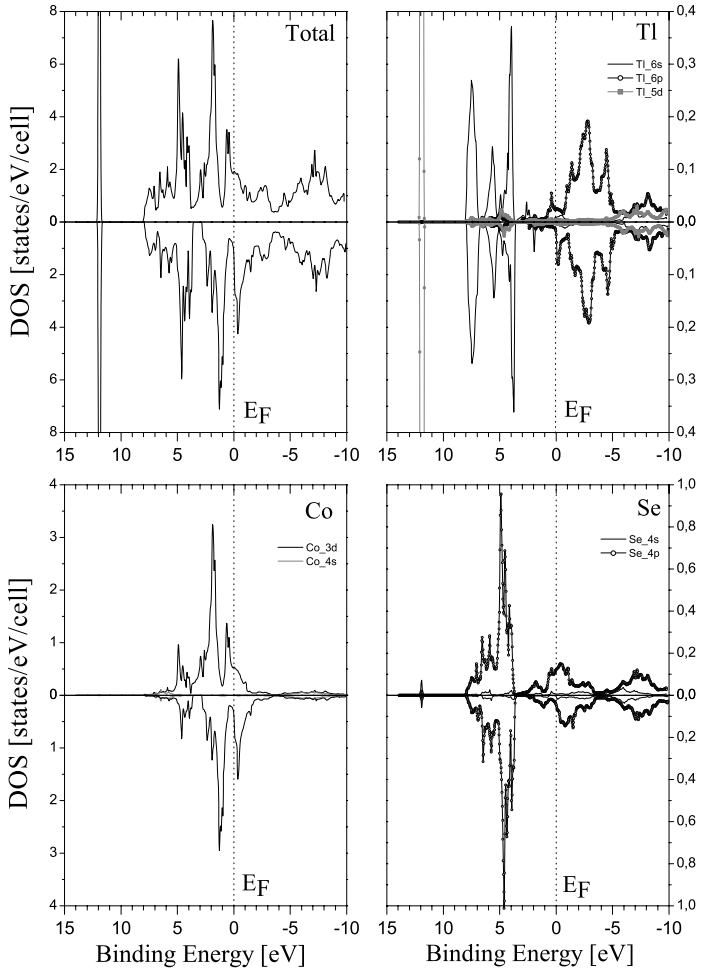

Figure 7. Spin-polarized Co, Se, Tl and total DOS calculations for ferromagnetic interactions within the cobalt layers computed by WIEN2k.

chemical conclusion drawn from this analysis is that the top of the valence band consists of states from Se 4p, mixed with Co 3d and to a very small extent Tl states, quite in line with expectation. That shows a picture of Tl with localized 6s states, conforming to the 'lone-pair' concept widely accepted for thallium and other heavy p-metals. Hence, the somewhat naive picture of describing the compound chemically as $Tl^{+}[T_2X_2]^{-}$ gets strong support [4].

4. Conclusions

$TlCo_2Se_2$ is confirmed to be metallic from XPS, RXES, resistivity and thermoelectric measurements and by our DOS calculations. The charge carriers are electron holes. The resistivity effects are anisotropic, indicating a two-dimensional character probably reflected in the temperature dependence of the Seebeck effect. The effect of Co–Se bonding is present through satellite features to the Co 2p XPS features. On changing the X element (X = S, Se), the bonding situation around Co would change, but sulfur and selenium are homovalent and of

almost the same electronegativity. The main bonding characteristics of $TlCo_2Se_2$ and $TlCo_2S_2$ appear to be very similar, not reflecting the strong difference in magnetic behaviour.

Different attempts [3, 15] have gained various success as to establishing the incommensurate helical magnetic structure of $TlCo_2Se_2$ as found by experiment. Even elaborate calculations presented in [3] and in figure 6 demanded experimental input. Fairly simple LMTO methods are able to demonstrate the energetic gain induced by spin-polarization, effectuated as the ferromagnetic ordering within the cobalt sheets of both $TlCo_2Se_2$ and $TlCo_2S_2$. However, the long-range effects are more difficult to treat, and there are at present no calculations to accompany the very interesting findings in the solid solutions $TlCo_2Se_{2-x}S_x$ where the helix structure prevails until near $x = 2$ but changes its pitch as a function of x [31]. Obviously, more sophisticated experiments or calculations must be implemented.

Acknowledgments

Funding by the Research Council of President of the Russian Federation (Grant NSH-4192.2006.2) and the Natural Sciences and Engineering Research Council of Canada (NSERC) and the Canada Research Chair Program is gratefully acknowledged. The work at the Advanced Light Source at Lawrence Berkeley National Laboratory was supported by US Department of Energy (Contract DE-AC03-76SF00098). Support was also provided by the Swedish Foundation for Strategic Research (SSF/FRAM).

We greatly appreciate the facilities put at our disposal by Professor T Palstra at the Materials Science Centre of the University of Groningen, allowing for the thermoelectricity measurements performed by Dr J Baas. We are grateful to Dr L Norén, at present at The Australian National University, Canberra, for furnishing us with the large crystals used in this work for various experiments. We are thankful to Dr A Postnikov for scientific advice concerning the calculations by the WIEN2k program and to Dr A A Syrtsov for performing preliminary calculations using LMTO code [32].

References

[1] Newmark A R, Huan G, Greenblatt M and Croft M 1989 *Solid State Commun.* **71** 1025–32
[2] Just G and Paufler P 1996 *J. Alloys Compounds* **232** 1–25
[3] Lizárraga R, Ronneteg S, Berger R, Bergman A, Mohn P, Eriksson O and Nordström L 2004 *Phys. Rev.* B **70** 024407
[4] Klepp K and Boller H 1978 *Monatsh. Chem.* **109** 1049–57
[5] Brun G, Gardes B, Tedenac J C, Raymond A and Maurin M 1979 *Mater. Res. Bull.* **14** 743–9
[6] Berger R and van Bruggen C F 1984 *J. Less-Comm. Met.* **99** 113–23
[7] Berger R 1989 *J. Less-Common Met.* **147** 141–8
[8] Berger R and van Bruggen C F 1985 *J. Less-Common Met.* **113** 291–323
[9] Huan G H, Greenblatt M and Ramanujachary K V 1989 *Solid State Commun.* **71** 221–8
[10] Huan G, Greaney M, Tsai P P and Greenblatt M 1989 *Inorg. Chem.* **28** 2448–51
[11] Greaney M, Huan G, Ramanujachary K V, Teweldemedhin Z and Greenblatt M 1991 *Solid State Commun.* **79** 803–10
[12] Norén L, Withers R L and Berger R 2000 *J. Solid State Chem.* **151** 260–6
[13] Broddefalk A, Nordblad P and Berger R 2000 *Physica* B **284** 1317–8
[14] Berger R, Fritzsche M, Broddefalk A, Nordblad P and Malaman B 2002 *J. Alloys Compounds* **343** 186–91
[15] Lizárraga R, Ronneteg S, Berger R, Mohn P, Nordström L and Eriksson O 2004 *J. Magn. Magn. Mater.* **272–276** 557–8
[16] Ronneteg S, Lumey M W, Dronskowski R, Gelius U, Berger R, Felton S and Nordblad P 2004 *J. Solid State Chem.* **177** 2977–84
[17] Gelius U, Wannberg B, Baltzer P, Fellner-Feldegg H, Carlsson G, Johansson C G, Larsson J, Munger P and Vegerfors G 1990 *J. Electron Spectrosc. Relat. Phenom.* **52** 747–85

[18] Jia J J, Callcott T A, Yurkas J, Ellis A W, Himpsel F J, Samant M G, Stöhr J, Ederer D L, Carlisle J A, Hudson E A, Terminello L J, Shuh D K and Perera R C C 1995 *Rev. Sci. Instrum.* **66** 1394–7
[19] Bearden J A 1967 *Rev. Mod. Phys.* **39** 78
[20] Sjöstedt E, Nordström L and Singh D 2000 *Solid State Commun.* **114** 15
[21] Sjöstedt E and Nordström L 2002 *Phys. Rev.* B **66** 014447
[22] von Barth U and Hedin L 1972 *J. Phys. C: Solid State Phys.* **5** 1629
[23] Singh D J 1994 *Planewaves, Pseudopotentials and the LAPW Method* (Boston, MA: Kluwer–Academic)
[24] Blaha P, Schwarz K, Madsen G K H, Kvasnicka D and Luitz J 2001 *WIEN2k,* Vienna University of Technology improved and updated Unix version of the original copyrighted WIEN code, which was published by Blaha P, Schwarz K, Sorantin P and Trickey S B 1990 *Comput. Phys. Commun.* **59** 339 URL http://www.wien2k.at
[25] Perdew J P, Burke K and Ernzerhof M 1996 *Phys. Rev. Lett.* **77** 3865–8
[26] Yeh J J and Lindau I 1985 *At. Data Nucl. Data Tables* **32** 1–155
[27] Galtayries A and Grimblot J 1999 *J. Electron Spectrosc. Relat. Phenom.* **99** 267–75
[28] Klebanoff L E, van Campen D G and Pouliot R J 1994 *Phys. Rev.* B **49** 2047–57
[29] van Campen D G and Klebanoff L E 1994 *Phys. Rev.* B **49** 2040–6
[30] Bearden J A and Burr A F 1967 *Rev. Mod. Phys.* **39** 125
[31] Ronneteg S, Felton S, Berger R and Nordblad P 2005 *J. Magn. Magn. Mater.* **299** 53–63
[32] Krier G, Jepsen O, Burkhardt A and Andersen O *The TB-LMTO-ASA program, version 4.7* Stuttgart, Germany Anderson O K, Jepson O and Sob M 1987 *Electronic Structure and its Applications* ed M S Yussouf (Berlin: Springer) p 2